MENINGEAL INFLAMMATION AND CORTICAL DEMYELINATION IN ACUTE MULTIPLE SCLEROSIS

Ryan J. Bevan, MSc[1], Rhian Evans, MSc[1], Lauren Griffiths, BSc[1], Lewis M. Watkins, MSc[1], Mark I. Rees, PhD, DSc[1], Roberta Magliozzi, PhD[2,5], Ingrid Allen, MBChB, DSc[3], Gavin McDonnell, MBChB[4], Rachel Kee, MBChB[4], Michelle Naughton, PhD[3], Denise C. Fitzgerald, PhD[3], Richard Reynolds, PhD[5], James W. Neal, MBChB, DPhil[1], Owain W. Howell, PhD[1,5]

[1]Institute of Life Sciences, Swansea University Medical School, Swansea. [2]Neurology Unit, University of Verona, Italy. [3]Wellcome-Wolfson Institute for Experimental Medicine, School of Medicine, Dentistry and Biomedical Science, Queen's University Belfast, Belfast. [4]Belfast Health and Social Care Trust, Belfast. [5]Division of Brain Sciences, Faculty of Medicine, Imperial College London, London.

Running head: Meningeal inflammation in acute MS

Word count (5003), 5 figures, 3 tables.

Corresponding author: Dr Owain W. Howell

Institute of Life Sciences (ILS1), Swansea University Medical School, Singleton Park Campus,

Swansea. UK. SA2 8PP.

Phone: ++44 (0)1792 295066

Email: o.w.howell@swansea.ac.uk

This article has been accepted for publication and undergone full peer review but has not been through the copyediting, typesetting, pagination and proofreading process, which may lead to differences between this version and the Version of Record. Please cite this article as doi: 10.1002/ana.25365

Abstract:

Objective: Cortical grey matter (GM) pathology, involving demyelination and neurodegeneration, associated with meningeal inflammation, could be important in determining disability progression in multiple sclerosis (MS). However, we need to know more about how cortical demyelination, neurodegeneration and meningeal inflammation contribute to pathology in early stages of MS to better predict long-term outcome.

Methods: Tissue blocks from short disease duration MS (n=12, median disease duration 2 years), progressive MS (n=21, disease duration 25 years), non-diseased controls (n=11) and other neurological inflammatory disease controls (n=6), were quantitatively analysed by immunohistochemistry, immunofluorescence and *in situ* hybridisation.

Results: Cortical GM demyelination was extensive in some cases of acute MS (range 1–48% of total cortical GM) and subpial lesions were the most common type (62%). The numbers of activated (CD68+) microglia/ macrophages were increased in cases with subpial lesions and the density of neurons was significantly reduced in acute MS normal appearing and lesion GM, compared to controls ($p<0.005$). Significant meningeal inflammation and lymphoid-like structures were seen in 4 of 12 acute MS cases. The extent of meningeal inflammation correlated with microglial/ macrophage activation ($p<0.05$), but not the area of cortical demyelination, reflecting the finding that lymphoid-like structures were seen adjacent to GM lesions as well as areas of partially demyelinated/remyelinated, cortical GM.

Interpretation: Our findings demonstrate that cortical demyelination, neuronal loss and meningeal inflammation are notable pathological hallmarks of acute MS and support the need to identify early biomarkers of this pathology to better predict outcome.

Introduction:

Multiple sclerosis (MS) is a highly variable and life-changing condition, characterised by inflammation, demyelination and neurodegeneration. MS typically presents as a relapsing-remitting disease, where bouts of acute inflammation and new, active, demyelinating lesions are associated with neurological impairment. Lesions of the grey matter (GM) occur at all stages of the disease and the extent of cortical GM pathology predicts conversion to clinically definite MS and associates with cognitive and motor disability, epilepsy and an earlier transition to the progressive phase[1].

Recent findings suggest that subpial GM lesions of the neocortex, the principal lesion type of the MS cortex, are related, at least in part, to inflammatory activity in the overlying leptomeninges[2]. We and others have shown how the degree of meningeal inflammation correlates with cortical microglial activation, neuritic and neuronal degeneration, and demyelination in primary progressive and secondary progressive MS[3–10]. Inflammatory cells of the leptomeninges (T- and B-lymphocytes, plasma cells and macrophages) are increased in number, can display a semi-organised lymphoid-like structure, and are typically seen in the deep cerebral sulci, but are also noted in the leptomeninges of the cerebellum and spinal cord[3,11,12].

Lymphoid-like structures (LLS), which can resemble ectopic B-cell follicles seen in other autoimmune diseases[13], are observed in models of MS and in approximately 40% of secondary progressive MS cases at post-mortem[5]. Cases of progressive MS harboring elevated leptomeningeal immune cell infiltration and LLS are associated with an early onset, shorter and more aggressive disease course, and accumulated disability more rapidly than those in which LLS could not be identified[5]. More recently, it has also been demonstrated that a signature of immune mediators important in lymphocyte homing and lymphoidogenesis, strongly predicts those people with early MS at risk of an extensive neocortical atrophy and MRI-visible cortical lesions[14].

We analysed a post-mortem cohort of MS cases with a short disease duration, who were diagnosed and died before the advent of disease modifying therapies. We asked the question if cortical lesions and neuronal loss are a feature of acute MS and if leptomeningeal inflammation is a notable pathological feature in the earliest stages of the clinical disease. These findings help us better understand the pathogenetic mechanisms of cortical GM pathology in early disease and may have implications for the rational identification of prognostic molecular and/or radiological measures for this heterogeneous condition.

Methods:

Cohort demographics: Human post-mortem tissue samples (South West Wales Research Ethics Committee approval #13/WA/0292) provided by the Thomas Willis Oxford Brain Bank and the Queen's University Belfast 'Dame Ingrid Allen Demyelinating Diseases' Tissue Collection were used to investigate the pathological features present in the earliest stages of MS. Cases of chronic progressive MS (primary and secondary progressive with disease duration >10 years) were provided by the UK MS Society Tissue Bank, Imperial College London (ethical approval #08/MRE09/31+5). Details of each case are listed in Table 1.

Six µm thick, formalin fixed paraffin embedded sections were cut from cerebral cortex and subcortical white matter blocks obtained from the superior frontal cortex, cingulate gyrus, occipital lobe and anterior hippocampus/para-hippocampal gyrus. Twelve cases of acute MS (9 female) were selected based on tissue availability and their short disease duration (median duration of 2 years (range 0.3y-4y), median age at death 35 years (range 22y-58y), Table 1). The cases of progressive MS represented a cohort of clinical and neuropathologically validated MS with evidence of active disease pathology, and comprised a minimum of three tissue blocks of frontal, cingulate and temporal cortex per case (primary progressive MS n=3, secondary progressive MS n=18, 12 female, median age at death 50 (range 38y-66y), disease duration 25yrs (range 10y- 39y)). Anatomically matched tissue blocks from eleven non-neurological disease controls were used for comparison. Control case selection was based on tissue availability, cause of death and the youngest possible age at death: age 56 years (range 41y-67y). In addition, we obtained tissue from six neuro-inflammatory disease controls; acute disseminated encephalomyelitis (n=1), cytomegalovirus encephalitis (n=3), neuromyelitis optica (n=1) and co-morbid meningoencephalitis with multiple sclerosis (n=1) for qualitative analysis (see Table 1).

Tissue characterisation and analysis: Tissue sections were stained with Luxol-Fast Blue and immunohistochemically stained with anti-proteolipid protein (PLP) and anti-CD68 antibodies to characterise demyelination and lesion inflammatory status, and parenchymal and meningeal connective tissue microglia/ macrophage density. Sections were assessed for the degree of grey and white matter demyelination, presence or absence of GM lesion types and presence of areas of tissue that appeared to be partially de/re-myelinated cortical GM. Cortical GM lesions were categorised following published criteria[15]: Type 1 or leucocortical GM lesions, type 2 or intracortical lesions, type 3 or subpial lesions, or type 4 or cortex spanning lesions. GM lesions displaying CD68+ microglia/ macrophage numbers equivalent to adjacent normal appearing GM were regarded as chronic inactive. Lesions with increased numbers of CD68+ microglial/ macrophage, typically restricted to the demyelinating lesion

edge and with evidence of PLP+ inclusions, were termed chronic active GM lesions. GM lesions with microglial/ macrophage activation throughout the lesion, and microglia/ macrophages containing inclusions of PLP+ material, were classified as active GM lesions.

White matter lesions were categorised based on their relative inflammatory activity, in accordance with previous descriptions[16,17]. White matter lesions were grouped as: (i) Active and demyelinating, displaying extensive CD68+ cells throughout the lesion with PLP+ inclusions within microglia/ macrophages; (ii) active and post-demyelinating, displaying extensive CD68+ cells but lacking PLP+ inclusions in microglia/ macrophages; (iii) chronic active lesions, displaying CD68+ cells at the lesion edge, often with evidence of active demyelination; and (iv) inactive lesions, with little increase in the number of CD68+ microglia/ macrophages at the lesion edge and no evidence of recent myelin phagocytosis. Fully remyelinated white matter lesions were classified as shadow plaques based on the 'normally appearing' PLP profile and classic Luxol Fast Blue 'shadow' appearance[18], whilst partial or incompletely remyelinated areas were referred to as remyelinating lesions. We acknowledge that the above characterisation only refers to the sampled area of incomplete lesions as present in standard histology sections[17].

The relative inflammatory status of cases was graded by assessing the degree of total cellular infiltration (Nissl counter-stained cellular infiltrates) of grey and white matter vessels and the meninges[5]. Briefly: absence or mild inflammation was rated 0+ (zero to 5 cells), diffuse and modest inflammation was rated ++ (equivalent to an infiltrate of 5–50 loosely packed cells in perivascular space or meninges); or more substantial infiltration was rated +++ (based on >50 cells in a tightly packed infiltrate, characteristic of a putative lymphoid-like structure).

Immunohistochemistry: Individual antibody details are listed in table 2. Briefly, following dewaxing, rehydration, epitope retrieval and blocking, slides were incubated with primary antibody overnight. Species-specific biotinylated secondary antibody (raised in horse or goat, Vector Laboratories, Peterborough, Cambridgeshire, UK) was applied and antibody binding visualised with the avidin-biotin-complex (ABC) peroxidase-linked reporter system, with 3, 3'-diaminobenzidine (DAB; Impact DAB; Vector Laboratories) as the chromogen. Tissue sections were counterstained with haematoxylin and DPX mounted. Dual colour immunohistochemistry was performed sequentially: Primary antibody 1 was detected using the IMPRESS-peroxidase detection kit (Vector), using DAB as the reporter chromogen. Primary antibody 2 was detected using the ABC- alkaline phosphatase detection system, using Vector Blue as the substrate. When using two primary antibodies raised in the same species (for dual CD20 and anti-PCNA), the slides were subjected to an additional round of

heat-retrieval in between the detection of primary antibody 1 and primary antibody 2, as described previously[19].

For immunofluorescence, relevant primary antibodies were amplified using the IMPRESS Dylight reaction kit (Vector Labs) or via biotin- streptavidin-fluorophore (Alexa 488 or Alexa 546) conjugates (MerckMillipore, Watford, UK). All sections were counterstained with 4',6-diamidino-2-phenylindole, dihydrochloride; DAPI (Sigma).

Images were acquired with a Zeiss Axio Imager M1 microscope and a Carl Zeiss AxioCam MRm monochrome camera (epifluorescence) or an AxioCam HRm (for brightfield microscopy). Negative controls were included and in all instances the relevant IgG control, or the absence of the secondary detection antibody, yielded no signal.

In situ hybridisation: In situ hybridisation (ISH) was performed using a 5' fluorescein (FAM)-labelled 19mer antisense oligonucleotide containing locked nucleic acid (LNA) and 2'-O-methyl (2'-O-Me)-RNA moieties in a 1:2 ratio. Probe design: Antisense C1QA (NM_015991) FAM- TggTccTugAugTuuCcuG and Sense FAM- CagGaaAcaTcaAggAccA; Antisense C3 (NM_000064) FAM- TagAaaGugAugGagAcuA and Sense FAM- AgaAauGauUggUggAuuA; Antisense CXCL13 (NM_006419) FAM- AuuGacTugTucTucTucC and Sense FAM-GgaAgaAgaAcaAguCaaT; (where capitals indicate LNA and lower case 2'-O-Methyl RNA in all instances; Eurogentec, Southampton, UK). ISH was performed as previously described[20,21] and hybridisation and wash conditions optimised so that all sense probes yielded essentially no signal. Appropriate sense probes and no probe controls were included in every experimental run. Specifically bound oligo-probe was visualised with a peroxidase conjugated goat anti-FAM (Vector) and DAB. For dual ISH and immunostaining, anti-HuC/D, anti-CD20 or anti-IBA-1 antibody binding was detected using appropriate horse anti-mouse or anti-rabbit biotin conjugated secondary and avidin-biotin-Alkaline Phosphate tertiary complex with Vector Blue substrate.

Quantitative morphometry: Histological or immunohistochemically stained tissue sections for LFB, PLP, CD68, CD3 and HuC/D were digitised by whole slide-scanning using a Leica SCF400F scanner. Image files were handled using QuPath[22]. To measure areas of demyelination, we first traced and measured the entire grey and white matter fraction for each LFB/haematoxylin stained slide using QuPath, before measuring the area of individual grey and white matter lesions on the serial PLP/haematoxylin stained section. Mean GM and white matter lesion area was reported per section and per case as the percentage of total grey or white matter, respectively. Using the 'Positive Cell Detection of a region of interest' tool in QuPath, a quantification of CD68+ microglia/ macrophages and HuC/D+ neurons was performed across the entire depth of the cortical ribbon- from the pial surface to the grey/

white matter boundary (count per mm^2 of the region of interest, minimum sampled area per region of interest= $2mm^2$). The number of parenchymal CD68+ microglia/ macrophages and the number of meningeal CD68+ macrophages and CD3+ T-cells (per mm of intact meninges), was determined.

Measuring myelin coverage and defining partially de/re-myelinated cortical grey matter: We used FIJI ImageJ (https://fiji.sc/) to determine the myelin coverage across the GM cortex in virtual x40 magnification PLP snapshots exported from QuPath (image size 2.25x 3.75mm). TIFF image snapshots were converted to greyscale before thresholding to mark all areas positive for anti-PLP specific immunostain. Myelin density profiles were generated for the entire depth of the cortical ribbon from areas of 'most normal' myelin and partially de/re-myelinated GM, in the same block and at the same architectonic point (i.e. sampled from base of sulcus or midway between sulcus and crown of gyrus) using the plot-profile selection tool. Myelin density profiles (captured in triplicate) were averaged and reported for every 2% step along the depth of the sampled cortex. Density profiles at each step were then compared relative to the same point in the myelin density profile of matched 'most normal' GM as described in the results and legend.

Statistical analysis: Results were presented as scatter dot plots with a line at the mean or as box and whiskers plots showing min-to-max values, interquartile range and group medians. Two-group comparisons were made using the Mann-Whitney U test or Wilcoxon matched pairs test, whilst three or more groups were compared by non-parametric one-way ANOVA (Kruskal-Wallis test), using Dunn's multiple comparisons post-test. Associations between pathological variables were tested by Spearman analysis (GraphPad PRISM v6).

Results:

Cortical grey and white matter demyelination in acute MS:

Anti-PLP immunostaining revealed extensive areas of white matter demyelination and all four cortical GM lesion types in acute MS (Fig 1A- D). Demyelinated cortical GM (as a percentage of total cortical GM) ranged from 1-48% (mean 11.9%, Fig 1E), whilst WM demyelination ranged from 2-81%. Average white matter lesion area was significantly greater than GM lesion area (34.3% versus 11.9%, p=0.0007) at this stage. Progressive MS cortex had three-times the extent of cortical GM demyelination as seen in acute MS (29.1% versus 11.9%, in progressive and acute MS, respectively, p=0.03), with the area of GM demyelination being comparable to that of white matter lesions in the same progressive MS cases (29.1% and 30.1%, for grey and white matter lesions, respectively).

Subpial (type 3) cortical GM lesions were the most abundant cortical GM lesion type in acute MS (seen twice as frequently as all other GM lesion types combined, Fig 1F). A number of small type 2 intracortical lesions were noted in acute MS (accounting for 19% of all cortical GM lesions). Interestingly, the proportion of type 3 GM lesions was remarkably similar in progressive MS but we failed to observe a single type 2 lesion in late disease. We noted an increase in the number of type 1 and type 4 GM lesion types (Fig 1F) in progressive cases.

Over 50% (36 of 69) of the GM lesions displayed signs of active demyelination (active or chronic active GM lesions, Fig 1G), with 12 of 69 GM lesions being categorised as fully active cortical GM lesions (being confluent in CD68+ microglia/ macrophages containing PLP+ inclusions; Figure 1H- K). Only chronic active and chronic inactive cortical GM lesions were seen in progressive MS. Those cases displaying type 3 cortical GM lesions had significantly elevated numbers of anti-CD68+ microglia/ macrophages across the full depth of the cortex, in comparison to those acute MS cases without type 3 lesions ($p=0.001$) or in comparison to non-neurological controls ($p=0.0002$; Fig 1L).

Neurodegeneration in acute MS:

A significant reduction in total HuC/D+ neuron density was observed in MS normal appearing GM (NAGM, 19.7% reduction, $p=0.0117$) and MS GM containing type 3 lesions (GML, 34.3% reduction, $p<0.0001$), in comparison to anatomically matched controls (Fig 2A, B).

We have previously shown that complement is activated in progressive MS GM neurons and complement activation correlated with severity of GM pathology[21,23], whilst others have shown complement C1q and C3b expression is associated with degenerating synapses in the progressive MS hippocampus[20]. We performed ISH for complement transcripts that encode the recognition fragment C1q and the central complement component C3. We saw evidence of, but did not quantify, complement transcript positive cells with a distinct neuronal morphology associated with IBA-1+ microglia (Figure 2C), C1QA and C3 transcript positive cells with a neuronal morphology (Fig 2D, E) and C1QA positive cells dual labeled with anti-HuC/D (Fig 2F, G).

White matter lesions in acute MS:

The majority of acute MS white matter lesions were classified as active inflammatory demyelinating lesions (Fig 3A- D), as might be expected for such a short disease duration cohort. Active white matter lesions accounted for 74% of all identified white matter lesions (39 lesions in total) in acute MS. The density of CD68+ microglia/ macrophages was

significantly elevated in active white matter lesions in comparison to chronic active lesions, remyelinating and/ or shadow plaques, normal appearing white matter (NAWM) and control white matter (Fig 3E, F).

Identification of leptomeningeal lymphoid-like structures (LLS) in acute MS:

Semi-quantitative analysis of the extent of perivascular and meningeal immune cell infiltrates revealed 4 of 12 acute MS cases with extensive (rated +++) leptomeningeal cell infiltrates. Cases with extensive perivascular and leptomeningeal infiltrates also contained a greater proportion of cortical GM lesions classified as active or chronic active, in comparison to chronic inactive (Fig 4A). These four cases accounted for 65% of all active and chronic active GM lesions seen in the acute MS cohort. LLS of the acute MS leptomeninges were associated with a widespread and elevated number of macrophages (CD68+), T-cells (CD3+) and B-cells (CD20+) throughout the preserved leptomeninges (Fig 4B- D). Dense aggregates of leptomeningeal immune cell infiltrates, containing CD20+ B-cells and CD3+ T-cells, were noted in these four cases (Fig 4E). CD8+ cytotoxic T-cells were evident in meningeal LLS (Fig 4F), along with B-cells co-expressing the marker of cell division PCNA, and leukocytes expressing transcripts of the key lymphogenic cytokine CXCL13 (Fig 4G, H).

The relationship between meningeal infiltrates, parenchymal microglial activation and myelin pathology in acute MS:

LLS in secondary progressive MS are typically associated with underlying areas of subpial cortical microglial activation and demyelination. Here we report a significant and robust association between the number of leptomeningeal macrophages and CD3+ lymphocytes (and a trend for CD20+ B-lymphocytes, r= 0.69, p= 0.07)) with the number of activated microglia/ macrophages in the subpial GM parenchyma in those acute MS cases with LLS (Table 3). It was interesting to note that alongside LLS, which were topographically associated with subpial GM lesions, we sometimes saw LLS next to areas of incompletely de/re-myelinated cortex (Fig 5A- H). Areas of partially de/re-myelinated cortical GM were identified based on a direct comparison to the most normal appearing GM in the same section to moderate the effect of the natural variation in myelination between cortical areas. We observed that the density of PLP+ immunostaining was reduced by up to 70% in the partially de/re-myelinated cortical GM in comparison to paired samples of adjacent NAGM. The area of significantly reduced PLP+ signal extended from the pia to almost halfway across the depth of the cortex (on average 48% of the distance from the pia to the grey/white matter border; Fig 5I). Within this same tissue, the number of parenchymal CD68+ microglia/ macrophages was significantly elevated in the partially de/re-myelinated cortical GM in comparison to matched samples of NAGM, whilst the number of meningeal CD68+

macrophages was increased in areas overlaying the affected cortical GM in comparison to the same areas of adjacent NAGM (Fig 5J, K). The number of CD3+ and CD20+ lymphocytes was unchanged in the meninges overlying the partially de/re-myelinated GM in comparison to normal GM (data not shown). Supporting the impression that the partially de/re-myelinated GM may represent, at least in part, a pathological change, we noted CD68+ microglia containing PLP+ inclusions of myelin and evidence of neurofilament-H+ neuritic transections and end-bulb like structures in the affected GM (Fig 5L- M).

Discussion:

We report that subpial cortical demyelination, neurodegeneration and widespread microglia/ macrophage activation, together with elevated meningeal inflammation and the presence of lymphoid-like structures, are notable pathological features in the earliest years since diagnosis in some acute MS cases. These data have implications for our understanding of the pathology underlying MS and support efforts to develop biomarkers of meningeal inflammation and cortical demyelination early in the disease, to aid the identification of those at risk of a more severe MS course.

Grey matter demyelination is widespread and active in acute MS:

The majority of neuropathological studies of cortical pathology have been conducted on cases of long-standing, progressive disease[2], and it has been suggested that the build-up of cortical damage may be more prominent at the later stages[9,10]. Here we analysed an archival cohort in what is, at present, the largest study of cortical pathology in acute MS. The cohort is defined by a short disease duration, which we have termed acute MS, and all patients died before the advent of effective anti-inflammatory therapies. Cases of such short disease duration are rare, given the success of current immunomodulatory therapies. Therefore, this tissue cohort provides an important resource for the description of cortical pathology, including demyelination, neurodegeneration and inflammation, in the early clinically apparent phase of the disease.

Cortical grey matter lesions, especially subpial (or type 3) GM lesions, were frequently noted in both our acute and progressive MS cohorts. Cortical pathology and significant subpial demyelination have also been documented in biopsy tissue taken as part of the diagnosis of MS with an atypical presentation[24]. In contrast to our study, Kutzelnigg *et al*, reported only modest cortical demyelination (0- 4% of total cortical GM measured from coronal macrosections) in a cohort of acute MS. Differences may partly be explained by the shorter

disease duration (up to 7 months compared to 4 years in this study), a younger age at death leading to a more aggressive cortical pathology in our cohort, or that our sampling of small blocks (1- 6 blocks per case) over-estimates what might be a highly variable pattern of cortical demyelination when viewed across the whole forebrain. However, these findings do suggest that the mechanisms that drive cortical lesion formation in acute MS may be the same as those that contribute to cortical pathology in long-term disease and are already present at an early stage. Subpial cortical lesion pathogenesis is associated with inflammation of the overlying leptomeninges[3,8,9]. Progressive cases with significant leptomeningeal inflammation at post-mortem had a gradient of neuronal, neuritic and glial cell loss[4], which are substrates for cortical thinning and atrophy measured by MRI[25]. High resolution T2* weighted MRI has highlighted that the greatest changes affect the outer 25% of the cortex in the earliest stage of the disease and that these signal changes are most significant in the sulci- a common site of subpial lesion pathology[5,26]. More generally, those patients with more cortical lesions and/or greater cortical atrophy, have greater cognitive dysfunction and attain disability milestones more rapidly[27–30], whilst cognitive and neuropsychiatric dysfunction are important indicators of cortical pathology even in the absence of classical MS clinical features[31]. Our finding of subpial lesions in a cohort who died following a short disease course supports a key role for cortical pathology in the disease outcome. This report adds weight to the recognised need to be able to detect subpial lesions *in vivo* so that we have a more complete picture of the patient's disease.

Numerous, small, intracortical lesions (type 2 lesions) were seen in early but not in progressive MS. Type 2 lesions are the least common cortical GM lesion and account for the smallest area of demyelination in progressive MS. The increased proportion of larger type 1 and type 4 lesions in later disease may account for this change- whereby the smaller type 2 lesions are subsumed as part of larger, neighbouring, lesions.

White matter lesions occupied a greater area than cortical grey matter lesions in acute MS, which could mean that white matter lesions are a dominant pathology site of injury in acute MS. It is important to note that the finding of significant WM demyelination may well reflect a selection bias in neuropathological studies. Selection of tissue blocks at initial brain dissection is typically based on the presence of macroscopically visible white matter lesions. Evidence for possible ascertainment bias is supported by our observation that WM lesion size was no different in later disease in samples selected based on anatomical region of interest rather than on available, visible, WM lesions. However, the suggested mechanisms involved in the formation of subpial lesions would mean that they are slower forming and might only accumulate over a longer period than acute white matter lesions. Our study was

principally focussed on cortical, and not WM, pathology in early MS. Subpial cortical GM lesions cannot be seen macroscopically, meaning that blocks cannot be pre-selected for this lesion type. In addition, there was no suggestion of an association between the extent of WM demyelination and GM demyelination in acute MS (Spearman r= 0.06, p= 0.91; comparing lesion area per block), meaning that any bias in block ascertainment should not bias our principal research findings.

Neurodegeneration occurs in the earliest years of the disease:

Earlier neuropathology studies have suggested that inflammation is accompanied by axonal and neuronal pathology at all stages of the disease[32]. In agreement with this, we noted extensive neuron loss in acute MS GM lesions and normal GM in comparison to matched non-diseased controls. The extent of neuron loss was comparable to that seen in the progressive MS cortex[4,6,21,33], and of a similar magnitude to other GM structures[34–36]. The significant neurodegeneration in acute MS is supported by evidence that the majority of neuron loss in the spinal cord occurs early in disease[37] and that in progressive MS the greatest neuronal loss is seen in those who experienced the shortest disease duration[2]. Neuronal stress and damage and eventual degeneration may be directly and/or indirectly driven by the local inflammation, perhaps as a consequence of serum protein leakage[38], the diffusion of cytotoxic mediators from the CSF-filled compartments[4,39], retrograde damage as a result of pathology along affected tracts[7], and oxidative damage as a consequence of inflammation[40] and/or mitochondrial dysfunction[41]. The density of activated (CD68+) tissue microglia/ macrophages was elevated in comparison to normal GM and control GM, which may cause, or be a consequence of, the neuron loss. Parenchymal T-cell infiltrates were noted, but were not quantitatively different between sampled regions (data not shown), whilst the number of parenchymal B-cells was negligible. These findings are different to those seen in some cortical GM lesions sampled *en passant* at biopsy, where significant parenchymal infiltrates were reported[24]. We believe this lack of compelling evidence for CD3+ T-cell or CD20+ B-cell infiltrates in the cortical parenchyma of cases with active GM lesions adds further weight to the important role that inflammation of the connective tissue, be it the perivascular space or meninges, might have in inducing local glial and neuronal damage and innate immune activation. Complement is a vital component of the innate immune system and complement over-activation sustains autoimmune disease. Complement activation is important in synaptic and neuritic destruction[42], and complement positive neurons are seen in MS and other neurological conditions[20,43–45]. Complement positive neurons show signs of stress/damage and are dysmorphic[21,23], and we show here that cortical neurons in acute MS express transcripts of key complement components. Therefore, not only is there significant focal neuronal loss but many surviving neurons express complement and are stressed or

damaged, although we cannot conclude that neuronal complement activation is causal or in consequence to the degenerative change.

Lymphoid-like structures (LLS) in MS cases of a short disease duration:
Meningeal inflammation in MS has been linked to demyelination of the spinal cord, cerebellum and forebrain[3,11,12] and similar subpial GM lesions can be induced by stereotactic injection of inflammatory cytokines into the leptomeningeal space of the rodent forebrain[39]. The meninges are an important site of antigen drainage, immune surveillance and inflammation, and ectopic lymphoid structures are commonly found in the connective tissues associated with other diseases of autoimmune or chronic inflammatory origin[13]. Such structures can be induced by T-follicular helper cells, cytokine networks and a changing stromal network of connective tissue cells, which may eventually support and sustain lymphocyte activation, B-cell selection and clonal expansion, and production of disease-relevant pathogenic antibodies and other soluble mediators[46].

In keeping with our previous studies demonstrating semi-organised immune cell infiltrates that can often resemble ectopic tertiary lymphoid tissues, we noted lymphoid-like structures in four of twelve acute MS cases; an incidence similar to that seen in progressive MS and in other organ-specific autoimmune diseases[5,13]. The finding of LLS in early MS suggests that the burden of injury and/or organ-specific immune signals necessary for LLS formation are evident from the earliest times in some MS cases. LLS formation and maintenance accompany elevated tissue damage and antigen release[46] and LLS+ early MS displayed a greater number of active cortical GM lesions, extensive neurodegeneration and elevated parenchymal microglia/ macrophage activation. Therefore, LLS could be an important sign of pathological disease activity at all stages of MS. In light of the above and because the presence of ectopic lymphoid tissues in synovial biopsies can stratify those in the early course of rheumatoid arthritis for treatment and is prognostic for outcome[47,48], there is a justifiable need to identify LLS and enhanced leptomeningeal inflammation in people with MS. Recent data suggests that a cytokine/chemokine signature of lymphoidogenesis is elevated in CSF of MS cases with more cortical lesions and greater meningeal inflammation at post-mortem, and the same immune mediators accurately identify those patients presenting with an elevated cortical pathology on MRI at disease onset[14]. Such a combined biological and radiological approach, coupled with measurable clinical variables[28], could therefore be more powerful in identifying those in the early stages of MS who are most at risk of a more severe disease course.

Areas of partially de/re-myelinated cortical grey matter and associated meningeal inflammation:

Together with an association with subpial cortical pathology, we noted that LLS were sometimes seen near areas of visibly reduced myelin density that may represent partially de/re-myelinated cortical GM. This affected GM was clearly not completely demyelinated GM, but was very different to region matched 'most' normal GM. The myelinated cortical GM in progressive MS displays significant synaptic, dendritic, axonal, neuronal and oligodendrocyte loss[4,8,25]. We noted that the partially de/re-myelinated GM contained increased numbers of activated microglia/ macrophages, microglia containing recently phagocytosed myelin debris, and damaged neurites. The cortical GM is efficiently remyelinated in MS and it's models[49] and is capable of repair following repeated episodes of demyelination[50], but GM remyelination is difficult to measure at post-mortem. It would be important to understand how the partially de/re-myelinated cortical GM associates with nearby demyelination and tract specific pathology and to what degree the affected tissue represents early demyelination, incomplete remyelination or partially demyelinated GM.

Alongside some of the limitations already discussed, we need to be cognisant of the fact that the study of demyelination in small tissue blocks is unlikely to represent the extent of pathology throughout the forebrain. Our findings may also be inadvertently biased in that our small blocks are sampled from brain regions which comprise some of the sites where cortical lesions are most frequently seen in later disease[5,9,10]. Tissue block sampling in this study was determined by the availability of suitable material. Additionally, we were unable to match controls and acute MS in terms of age at death (Table 1). Age is an important determinant of total neuron number in the adult brain[51] and our findings of significant neuron loss in a younger cohort may have been underestimated.

To conclude, we show that meningeal inflammation, neurodegeneration, cortical demyelination and a partially de/re-myelinated grey matter are notable pathological features of acute MS. Our results suggest that all of these pathologies may begin very early on in the clinical disease course and can already be substantial after 2 years since diagnosis. By combining biomarkers of intrathecal inflammation and neurodegeneration, together with the most sensitive imaging methods, it may yet be possible to predict those newly diagnosed with MS who are most at risk of early cortical pathology and the associated cognitive and motor disability, and therefore most in need of aggressive immunotherapy, for the best long-term outcome.

Acknowledgements:

We would like to thank Dr Djordje Gveric and the team of the UK MS Society Tissue Bank (The Multiple Sclerosis Society Tissue Bank is funded by the Multiple Sclerosis Society of Great Britain and Northern Ireland (registered charity 207495)), and Drs Carolyn Sloan and Marie Hamard at the Oxford Brain Bank (supported by the Medical Research Council, Brains for Dementia Research, Alzheimer Society and Alzheimer Research UK, Autistica UK and the NIHR Oxford Biomedical Research Centre). Funding for this project was from the St. David's Medical Foundation, British Neuropathological Society, the MacDaid Scholarship, the Life Sciences Research Network Wales (RB, RE, LW, OH) and the MS Society (RR).

Author contributions: RB, RR, JN, OH contributed to the conception and design of the study. RB, RE, LG, LW, MR, RM, GM, RK, IA, MN, DF, OH contributed to the acquisition and analysis of data. RB, RR, JN, OH contributed to drafting the text and preparing the figures.

Potential conflict of interest:

None of the authors has a conflict of interest related to this study.

References:

1. Calabrese M, Magliozzi R, Ciccarelli O, et al. Exploring the origins of grey matter damage in multiple sclerosis. Nat. Rev. Neurosci. 2015;16(3):147–158.
2. Reynolds R, Roncaroli F, Nicholas R, et al. The neuropathological basis of clinical progression in multiple sclerosis. Acta Neuropathol. 2011;122(2):155–70.
3. Serafini B, Rosicarelli B, Magliozzi R, et al. Detection of ectopic B-cell follicles with germinal centers in the meninges of patients with secondary progressive multiple sclerosis. Brain Pathol. 2004;14(2):164–74.
4. Magliozzi R, Howell OW, Reeves C, et al. A Gradient of neuronal loss and meningeal inflammation in multiple sclerosis. Ann. Neurol. 2010;68(4):477–93.
5. Howell OW, Reeves CA, Nicholas R, et al. Meningeal inflammation is widespread and linked to cortical pathology in multiple sclerosis. Brain 2011;134(Pt 9):2755–71.
6. Choi SR, Howell OW, Carassiti D, et al. Meningeal inflammation plays a role in the pathology of primary progressive multiple sclerosis. Brain 2012;135(Pt 10):2925–37.
7. Haider L, Zrzavy T, Hametner S, et al. The topograpy of demyelination and neurodegeneration in the multiple sclerosis brain. Brain 2016;139(Pt 3):807–15.
8. Magliozzi R, Howell O, Vora A, et al. Meningeal B-cell follicles in secondary

progressive multiple sclerosis associate with early onset of disease and severe cortical pathology. Brain 2007;130(Pt 4):1089–104.

9. Kutzelnigg A, Lucchinetti CF, Stadelmann C, et al. Cortical demyelination and diffuse white matter injury in multiple sclerosis. Brain 2005;128(Pt 11):2705–12.
10. Kutzelnigg A, Lassmann H. Cortical demyelination in multiple sclerosis: A substrate for cognitive deficits? J. Neurol. Sci. 2006;245(1–2):123–126.
11. Androdias G, Reynolds R, Chanal M, et al. Meningeal T cells associate with diffuse axonal loss in multiple sclerosis spinal cords. Ann. Neurol. 2010;68(4):465–76.
12. Howell OW, Schulz-Trieglaff EK, Carassiti D, et al. Extensive grey matter pathology in the cerebellum in multiple sclerosis is linked to inflammation in the subarachnoid space. Neuropathol. Appl. Neurobiol. 2015;41(6):798–813.
13. Pitzalis C, Jones GW, Bombardieri M, Jones SA. Ectopic lymphoid-like structures in infection, cancer and autoimmunity. Nat. Rev. Immunol. 2014;14(7):447–462.
14. Magliozzi R, Howell OW, Nicholas R, et al. Inflammatory intrathecal profiles and cortical damage in multiple sclerosis. Ann. Neurol. 2018;83(4):739–755.
15. Bø L, Vedeler C a, Nyland HI, et al. Subpial demyelination in the cerebral cortex of multiple sclerosis patients. J. Neuropathol. Exp. Neurol. 2003;62(7):723–732.
16. Lassmann H, Raine CS, Antel J, Prineas JW. Immunopathology of multiple sclerosis: report on an international meeting held at the Institute of Neurology of the University of Vienna. J. Neuroimmunol. 1998;86(2):213–7.
17. Kuhlmann T, Ludwin S, Prat A, et al. An updated histological classification system for multiple sclerosis lesions. Acta Neuropathol. 2016;133(1):13–24.
18. Prineas JW, Barnard RO, Kwon EE, et al. Multiple sclerosis: remyelination of nascent lesions. Ann. Neurol. 1993;33(2):137–51.
19. Bauer J, Lassmann H. Neuropathological Techniques to Investigate Central Nervous System Sections in Multiple Sclerosis. Methods Mol. Biol. 2014;1304:211–29.
20. Michailidou I, Willems JGP, Kooi E-J, et al. Complement C1q-C3-associated synaptic changes in multiple sclerosis hippocampus. Ann. Neurol. 2015;77(6):1007–1026.
21. Watkins LM, Neal JW, Loveless S, et al. Complement is activated in progressive multiple sclerosis cortical grey matter lesions. J. Neuroinflammation 2016;13(1):161.
22. Bankhead P, Loughrey MB, Fernández JA, et al. QuPath: Open source software for digital pathology image analysis. Sci. Rep. 2017;7(1):16878.
23. Loveless S, Neal JW, Howell OW, et al. Tissue microarray methodology identifies complement pathway activation and dysregulation in progressive multiple sclerosis. Brain Pathol. 2018;28(4):507–520.
24. Lucchinetti CF, Popescu BFG, Bunyan RF, et al. Inflammatory cortical demyelination in early multiple sclerosis. N. Engl. J. Med. 2011;365(23):2188–97.

25. Popescu V, Klaver R, Voorn P, et al. What drives MRI-measured cortical atrophy in multiple sclerosis? Mult. Scler. 2015;21(10):1280–90.
26. Mainero C, Louapre C, Govindarajan ST, et al. A gradient in cortical pathology in multiple sclerosis by in vivo quantitative 7 T imaging. Brain 2015;138(4):932–945.
27. Calabrese M, Romualdi C, Poretto V, et al. The changing clinical course of multiple sclerosis: a matter of gray matter. Ann. Neurol. 2013;74(1):76–83.
28. Scalfari A, Romualdi C, Nicholas RS, et al. The cortical damage, early relapses, and onset of the progressive phase in multiple sclerosis. Neurology 2018;90(24):e2107–e2118.
29. Calabrese M, Agosta F, Rinaldi F, et al. Cortical Lesions and Atrophy Associated With Cognitive Impairment in Relapsing-Remitting Multiple Sclerosis. Arch Neurol 2009;66(9):1144–1150.
30. Harrison DM, Roy S, Oh J, et al. Association of Cortical Lesion Burden on 7-T Magnetic Resonance Imaging With Cognition and Disability in Multiple Sclerosis. JAMA Neurol. 2015;21201:1–9.
31. Zarei M, Chandran S, Compston A, Hodges J. Cognitive presentation of multiple sclerosis: Evidence for a cortical variant. J. Neurol. Neurosurg. Psychiatry 2003;74(7):872–877.
32. Frischer JM, Bramow S, Dal-Bianco A, et al. The relation between inflammation and neurodegeneration in multiple sclerosis brains. Brain 2009;132(Pt 5):1175–89.
33. Carassiti D, Altmann DR, Petrova N, et al. Neuronal loss, demyelination and volume change in the multiple sclerosis neocortex. Neuropathol. Appl. Neurobiol. 2018;44(4):377–390.
34. Cifelli A, Arridge M, Jezzard P, et al. Thalamic neurodegeneration in multiple sclerosis. Ann. Neurol. 2002;52(5):650–3.
35. Vercellino M, Masera S, Lorenzatti M, et al. Demyelination, inflammation, and neurodegeneration in multiple sclerosis deep gray matter. J. Neuropathol. Exp. Neurol. 2009;68(5):489–502.
36. Papadopoulos D, Dukes S, Patel R, et al. Substantial archaeocortical atrophy and neuronal loss in multiple sclerosis. Brain Pathol. 2009;19(2):238–53.
37. Schirmer L, Albert M, Buss A, et al. Substantial early, but nonprogressive neuronal loss in multiple sclerosis (MS) spinal cord. Ann. Neurol. 2009;66(5):698–704.
38. Yates RL, Esiri MM, Palace J, et al. Fibrin(ogen) and neurodegeneration in the progressive multiple sclerosis cortex. Ann. Neurol. 2017;82(2):259–270.
39. Gardner C, Magliozzi R, Durrenberger PF, et al. Cortical grey matter demyelination can be induced by elevated pro-inflammatory cytokines in the subarachnoid space of MOG-immunized rats. Brain 2013;136(12):3596–3608.

40. Haider L, Fischer MT, Frischer JM, et al. Oxidative damage in multiple sclerosis lesions. Brain 2011;134(Pt 7):1914–24.
41. Campbell G., Ziabreva I, Reeve A., et al. Mitochondrial DNA deletions and neurodegeneration in multiple sclerosis. Ann. Neurol. 2011;69(3):481–92.
42. Hong S, Beja-Glasser VF, Nfonoyim BM, et al. Complement and microglia mediate early synapse loss in Alzheimer mouse models. Science 2016;352(6286):712–716.
43. Ingram G, Loveless S, Howell OW, et al. Complement activation in multiple sclerosis plaques: an immunohistochemical analysis. Acta Neuropathol. Commun. 2014;2(1):53.
44. Lobsiger CS, Boillee S, Cleveland DW. Toxicity from different SOD1 mutants dysregulates the complement system and the neuronal regenerative response in ALS motor neurons. Proc. Natl. Acad. Sci. 2007;104(18):7319–7326.
45. Yasojima K, Schwab C, McGeer EG, McGeer PL. Up-regulated production and activation of the complement system in Alzheimer's disease brain. Am. J. Pathol. 1999;154(3):927–936.
46. Jones GW, Jones SA. Ectopic lymphoid follicles: Inducible centres for generating antigen-specific immune responses within tissues. Immunology 2016;147(2):141–151.
47. Klaasen R, Thurlings RM, Wijbrandts CA, et al. The relationship between synovial lymphocyte aggregates and the clinical response to infliximab in rheumatoid arthritis: A prospective study. Arthritis Rheum. 2009;60(11):3217–3224.
48. Cañete JD, Celis R, Moll C, et al. Clinical significance of synovial lymphoid neogenesis and its reversal after anti-tumour necrosis factor alpha therapy in rheumatoid arthritis. Ann. Rheum. Dis. 2009;68(5):751–6.
49. Albert M, Antel J, Brück W, Stadelmann C. Extensive cortical remyelination in patients with chronic multiple sclerosis. Brain Pathol. 2007;17(2):129–138.
50. Rodriguez EG, Wegner C, Kreutzfeldt M, et al. Oligodendroglia in cortical multiple sclerosis lesions decrease with disease progression, but regenerate after repeated experimental demyelination. Acta Neuropathol. 2014;128(2):231–46.
51. Pakkenberg B, Gundersen HJG. Neocortical Neuron Number in Humans: Effect of Sex and Age. J. Comp. Neurol. 1997;384:312–320.

Legends:

Figure 1. Cortical demyelination in acute MS. Tissue from individuals with MS that died following a short disease duration (n=12) presented with cortical and subcortical lesions identified by anti-PLP immunostaining (A- D, arrows point to lesion edge). Cortical demyelination was variable and sometimes extensive in acute MS (E), whilst subpial cortical demyelination (type 3 cortical lesions) were seen most frequently (F). More cortical grey matter lesions were classified as active or chronic active in acute MS in comparison to progressive MS (G). Cortical demyelination was accompanied by microglia/ macrophage activation (CD68+; H, I; active and chronic active GM lesions, respectively), evidence of recent myelin phagocytosis (arrows highlighting PLP inclusions in IBA-1+ microglia/ macrophages, J- active GM lesion, K- chronic active GM lesion) and an overall increase in cortical microglia/ macrophages in acute MS normal and demyelinated grey matter in comparison to non-disease controls (L). Groups were compared by non-parametric Kruskal-Wallis test with Dunn's post-test. *= $p<0.01$, ***= $p<0.0001$. Abbreviations; Ctrl, control; GM, grey matter; GML, grey matter lesion; NAGM, normal appearing GM; WM, white matter; A, active inflammatory lesion; CA, chronic active inflammatory lesion; CI, chronic inactive inflammatory lesion. Scale bars, A- D= 5mm; H, I= 50µm; J, K= 5µm.

Figure 2. Neurodegeneration in acute MS. The density of cortical HuC/D+ neurons was significantly reduced in normal appearing grey matter (NAGM) and lesion grey matter (GML) in comparison to matched control grey matter (Ctrl; A and B). We observed, but did not quantify, cells of acute MS cortex that expressed transcripts for the complement recognition protein C1Q, which were in close proximity to IBA-1+ microglia (C, arrow), C1QA and C3 mRNA positive cells with a neuronal morphology (D, E), co-labeled with anti- HuC/D sera (F, HuC/D, highlighted by the arrow), whilst sense transcripts processed as part of the same experimental run were negative (G). Kruskal-Wallis test with Dunn's post-test. *= $p<0.01$, ***= $p<0.0001$, multiplicity adjusted p values quoted in the main text. Scale bars; B= 100µm, C, F, G= 20µm, D, E= 50µm.

Figure 3. Inflammatory demyelination of the acute MS white matter. MS white matter lesions were classified as active inflammatory demyelinating lesions (A, A', B, B' anti-PLP immunostaining, A'', B'', anti-CD68), and further described as active white matter lesions with evidence of recent myelin phagocytosis (active and demyelinating (C, D, arrows showing IBA-1+ macrophages laden with anti-PLP positive material) and those lacking evidence of recent myelin phagocytosis (active and post-demyelinating; B). Active white matter lesions accounted for 74% of all identified white matter lesions (WM T), with chronic

active (CA) lesions and remyelinating and/or shadow plaque lesions (RM/Sdw) less frequently observed (E). The density of CD68+ microglia/ macrophages reflected the state of active inflammation in early disease (F). Kruskal-Wallis and Dunn's post-test. *= $p<0.01$, **= $p<0.01$, ***= $p<0.0001$. Scale bars; A, B= 200µm; A'- B'', C, D= 50µm.

Figure 4. Meningeal inflammatory infiltrates and lymphoid-like structures in acute MS. We scored the number of blocks harboring lymphoid-like structures (LLS) and rated the diffuse cellular infiltration of the meninges and parenchymal vessels (A). Four of 12 cases displayed evidence of meningeal LLS and contained areas of elevated connective tissue inflammation (meningeal/ perivascular inflammation). Active cortical GM lesions (red), and chronic active GM lesions (dark grey), were noted in the LLS+ cases, whilst inactive GM lesions (light grey) were enriched in the cases lacking observable LLS or connective tissue infiltrates. LLS+ cases had significantly elevated numbers of meningeal CD68+ monocytes (B), CD3+ T-cells (C) and CD20+ B-cells (D) in comparison to LLS- and control cases (cells per mm length of meninges). Representative example of meningeal LLS containing CD20+ B-cells and CD3+ T-cells identified in case D192 (E). A LLS from case C0069 demonstrating the presence of CD8+ T-cells (F, red). LLS of the meninges contained dividing B-cells (CD20/PCNA+, G and inset with arrow) and CXCL13 transcript positive cells as part of a CD20+ immunostained meningeal infiltrate (H, with boxed areas captured at higher magnification. Arrows identify CXCL13+ ISH signal). Kruskal-Wallis and Dunn's post-test. *= $p<0.05$, **= $p<0.01$, ***= $p<0.0001$.Scale bars: E, G, H= 100µm; F= 20µm.

Figure 5. Characterising areas of partially de/re-myelinated cortical grey matter in acute MS. LLS were seen next to subpial cortical lesions and areas of partially de/re-myelinated, but not fully demyelinated, grey matter (A, B; arrowhead indicates meningeal infiltrate and arrows indicate PLP+ lesion edge). Areas of partially de/re-myelinated cortical GM PLP+ myelin were visibly different to normal appearing GM in the same block (C- normal, D- affected GM) and line histograms were plotted in triplicate per region of normal or partially de/re-myelinated GM per case following image transformation and thresholding (E-H). Myelin coverage was averaged and reported for each 2% increment from the pia to the grey- white matter border and plotted relative to the 'most normal' grey matter measures taken from the same tissue block (I). Quantification revealed myelin coverage to be reduced by approximately 70% in the outer laminae in comparison to matched normal GM from the same block ($p<0.05$). Areas of quantitatively identified partially de/re-myelinated cortical GM (labeled as affected GM) displayed elevated numbers of parenchymal CD68+ microglia/ macrophages and were associated with elevated numbers of CD68+ macrophages in the overlying meninges (J, K). Areas of partially de/re-myelinated cortical GM containing

microglia with inclusions of PLP (L; dual IHC for IBA-1 and PLP. L'- L'' are higher resolution images from the partially de/re-myelinated area shown and arrows highlight IBA-1+ cells with PLP+ inclusions) and evidence of neurite damage (M, arrow highlights a neuritic end-bulb stained with anti-neurofilament-H). Unpaired t test, one per row, corrected for multiple comparisons using the Holm-Sidak method (I) or two-group comparisons using the Wilcoxon matched pairs test (J, K). Scale bars: A-F, 3mm; L= 100µm; M= 20µm.

Table 1:

Acute MS	*Disease*	*Gender*	*Disease Duration, yr*	*Age at Death, yr*	*Cause of Death*	*Available Blocks*
B8442	Acute MS	F	<2	29	Bronchopneumonia	4
B9860	Acute MS	F	2	53	Respiratory infection	6
C0069	RRMS	F	0.3	26	Bronchopneumonia	4
B5781	SPMS	F	2.7	37	Pulmonary embolism and inhalation pneumonia	3
D248	Acute MS	F	<2	40	Pulmonary congestion	2
D150	PPMS	F	<2	23	Lung abscess, bronchopneumonia	2
D147	Acute MS	F	<2	33	Severe MS, pulmonary embolus with abscess	3
D192	Acute MS	F	0.3	22	Hypoxic injury	5
D134	RRMS	F	4	41	Bronchopneumonia and pulmonary embolus	5
D140	Acute MS	M	2	58	Sepsis	3
D160	Acute MS	M	2	51	Acute attack	1
D200	Acute MS	M	<4	31	Focal haemorrhage	3
N=12		***9 F***	***2 yr***	***35 yr***		

Prog MS	*Disease*	*Gender*	*Disease Duration, yr*	*Age at Death, yr*	*Cause of Death*	*Available Blocks*
MS402	SPMS	M	20	46	MS, bronchopneumonia	4
MS405	SPMS	M	25	62	MS, septicaemia, metastatic colon cancer	4
MS407	SPMS	F	19	44	Septicaemia, pneumonia	3
MS408	SPMS	M	10	39	Pneumonia, sepsis	4
MS422	SPMS	M		58	Chest infection due to MS	4
MS423	SPMS	F	30	54	Pneumonia	4
MS425	SPMS	F	21	46	Pneumonia, MS	3
MS438	SPMS	F	18	53	MS	4
MS461	SPMS	M	21	43	Broncopneumonia	3
MS485	PPMS	F	29	57	Bronchopneumonia, MS	4
MS491	SPMS	F	26	64	Anaphylactic reaction	4
MS492	PPMS	F	31	66	Sigmoid cancer	4
MS497	SPMS	F	29	60	Aspiration pneumonia, MS	4
MS510	SPMS	F	22	38	Pneumonia, MS	4
MS513	SPMS	M	18	51	MS, respiratory failure	4
MS517	PPMS	F	25	48	Sepsis, MS	3
MS523	SPMS	F	32	63	Bronchopneumonia, MS	3
MS527	SPMS	M	25	47	Pneumonia, MS	4
MS528	SPMS	F	25	45	MS	3
MS530	SPMS	M	24	42	MS	4
MS538	SPMS	M	39	50	Pneumonia	3
N=21	***18 SPMS***	***12 F***	***25 yr***	***50 yr***		

NID control	***Disease***	***Gender***	***Disease Duration, yr***	***Age at Death, yr***	***Cause of Death***	***Available Blocks***
D095	Meningoencephalitis & Acute MS	F	n/d	39	Meningoencephalitis & ovarian tumour	1
91/1343	CMV	M	n/d	32	Bronchopneumonia	1
C4178	CMV	M	n/d	59	CMV	1
D255	CMV	M	n/d	32	Hypoxic injury	1
NP13/047	ADEM	M	n/d	26	Pulmonary embolism	1
RI06/166	NMO	F	n/d	18	Respiratory obstruction	1
N=6		***2 F***		***32 yr***		***1***

Control	***Disease***	***Gender***	***Disease Duration, yr***	***Age at Death, yr***	***Cause of Death***	***Available Blocks***
NP011/13	n/a	F	n/a	62	Metastatic colorectal cancer	2
NP012/13	n/a	F	n/a	60	Metastatic breast cancer	2
NP103/13	n/a	F	n/a	48	End-stage interstitial lung disease	2
NP039/13	n/a	M	n/a	41	Myocardial infarct	2
NP126/13	n/a	M	n/a	56	Cardiac arrest	2
NP127/13	n/a	M	n/a	60	Cardiac arrest	2
NP11/093	n/a	F	n/a	52	Chronic Liver Disease	2
NP1231/93	n/a	M	n/a	58	-	2
NP12/088	n/a	M	n/a	51	Cardiac arrest	2
NP12/052	n/a	F	n/a	42	Metastatic pancreatic carcinoma	2
NP12/132	n/a	F	n/a	67	-	2
N=11		***6 F***		***56 yr***		

Table 1: Details of acute, progressive (Prog) multiple sclerosis, other neuroinflammatory disease controls (NID) and non-neurological controls (controls) used in this study. Acute MS defines a cohort of short disease duration and included retrospectively confirmed cases of: acute MS (n=8), relapsing remitting MS (n=2), secondary progressive (SP) MS (n=1) and primary progressive (PP) MS (n=1). Median age of death and disease duration is shown where applicable. 'Available blocks' indicates the number of unique brain tissue blocks analysed per case. Abbreviations; ADEM, acute disseminated encephalomyelitis; CMV, cytomegalovirus encephalitis; F, female; n/a, not applicable; n/d, not determined; NMO, neuromyelitis optica; M, male; yr, years.

Table 2:

Antibody (anti-)	*Target*	*Source*	*Type/Clone*	*Dilution*
PLP	Proteolipid protein myelin	Abd Serotec	mAb/plpc1	1:2000
CD68	CD68+ microglia/ macrophages	Dako Cytomation	mAb/KP1	1:400
CD3	T-cells	Dako Cytomation	Rabbit pc	1:1200
CD20	B-cells	Dako Cytomation	mAb/L26	1:125
CD8	CD8+ T-cells	Dako Cytomation	C8-144B	1:100
IBA-1	Aallograft inflammatory factor. Microglia/ macrophages	FUJIFILM Wako Chemicals	Rabbit pc	1:2000
HuC/D	Human HuC/D neuronal protein	ThermoFisher	mAb/ 16A11	1:2000
NFil	Neurofilament 200kDa	Merck Millipore	mAb/ RT-97	1:1000
PCNA	Proliferating cell nuclear antigen	Dako Cytomation	mAb/ PC10	1:1000

Table 2: Primary antibodies used in this study. Antibody name, target cell, commercial source and working dilution are listed. Abbreviations; mAb, monoclonal mouse antibody; pc, polyclonal antibody.

Table 3:

	Meningeal CD68+ (cells/ mm)	***Meningeal CD3+ (cells/ mm)***	***Meningeal CD20+ (cells/ mm)***	***Total Meningeal infiltrate (cells/ mm)***
LLS+ parenchymal CD68 (cells/ mm^2)	r=0.8810 p= 0.0072	r= 0.8571 p=0.0107	r= 0.6905 p= 0.0694	r= 0.8089 p= 0.0276
LLS- parenchymal CD68 (cells/ mm^2)	r= 0.3427 p= 0.2762	r= 0.6434 p=0.0278	r= 0.4297 p=0.2821	r= 0.6071 p= 0.1667
LLS+ GML area (% total GM)	r= 0.1818 p= 0.5950	r= 0.500 p= 0.1217	r= 0.6515 p= 0.0340	r= 0.5364 p= 0.0939
LLS- GML area (% total GM)	r= 0.1429 p= 0.7825	r= 0.3214 p= 0.4976	r= -0.200 p= 0.9167	r= 0.400 p= 0.7500

Table 3. Relationships between meningeal inflammation (column headings) and parenchymal microglia/ macrophage density or grey matter lesion (GML) area in lymphoid-like structure positive (LLS+) or negative (LLS-) cases. Significant associations are underlined (Spearman analysis).

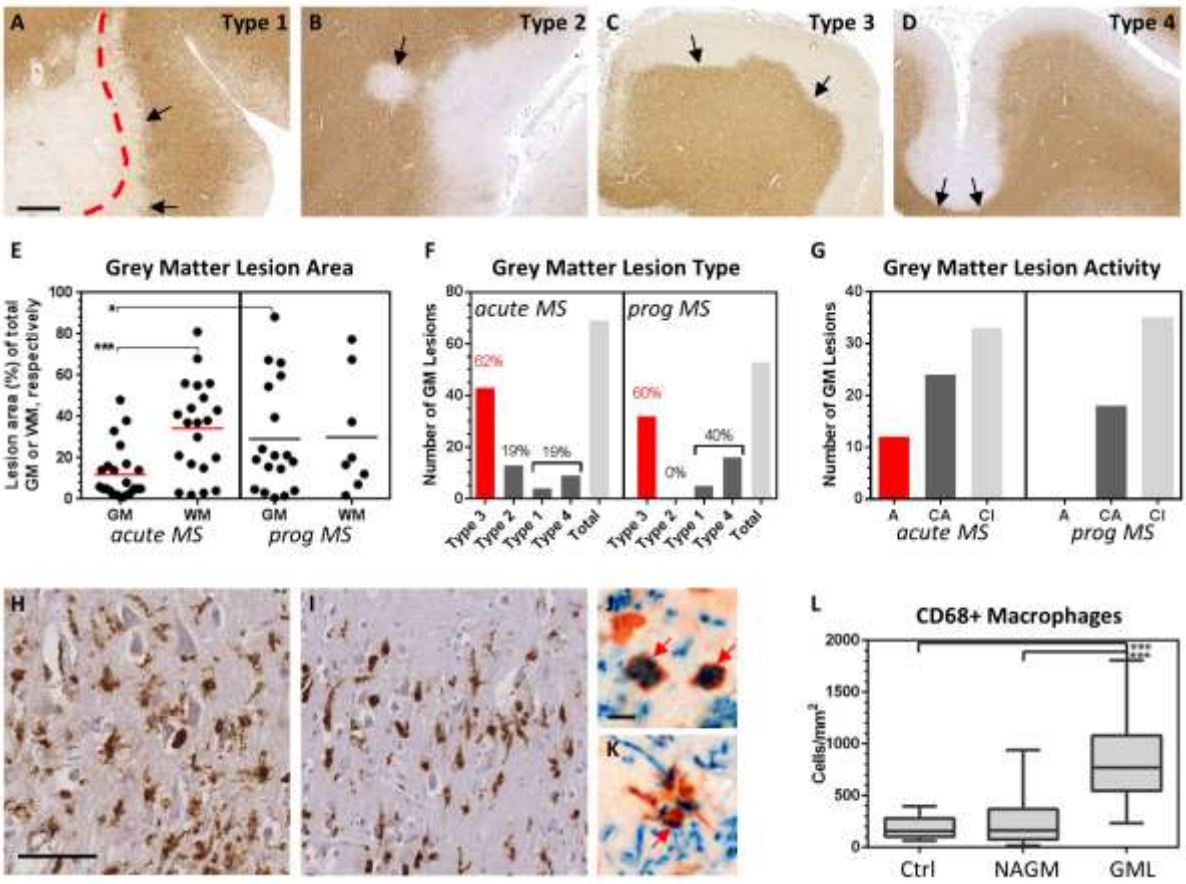

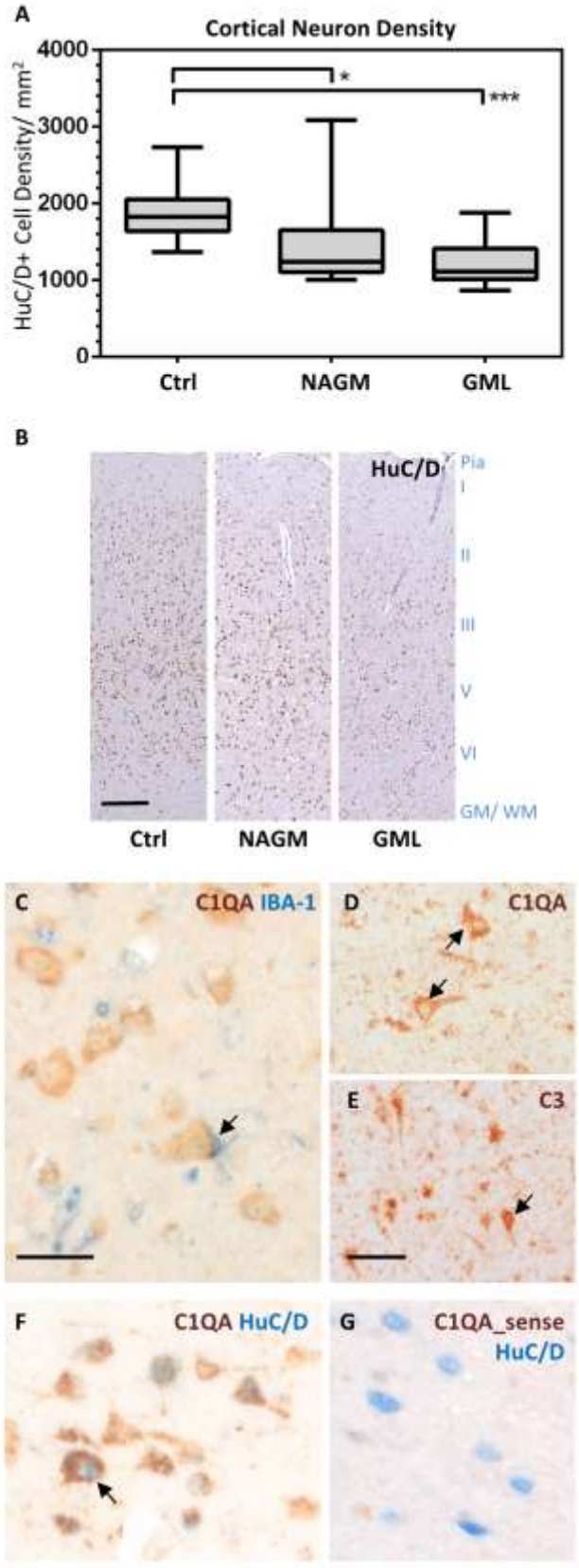

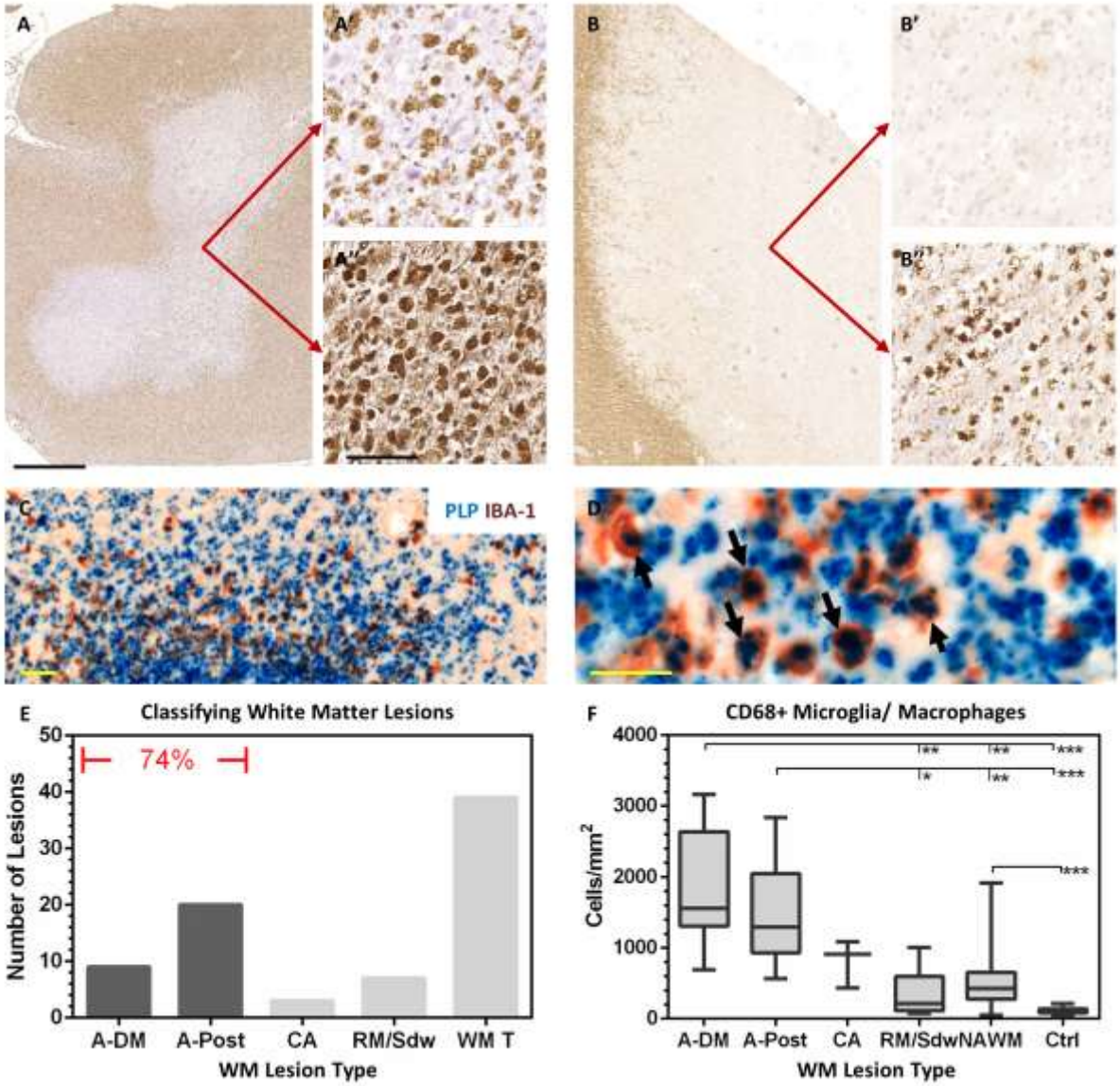

A

Case	Tissue Blocks with LLS/Examined Blocks (Number of LLS)	Meningeal/ P'vas Inflammation GM	Proportion of Lesion Activity
B9860	2/6 (4)	+++/++	
D192	4/5 (6)	+++/++	
D160	1/1 (2)	+++/++	
C0069	1/4 (1)	+++/+	
B5781	0/3	+/++	
B8442	0/4	+/+	
D200	0/3	0/+	
D134	0/5	0/+	
D140	0/3	0/+	
D147	0/3	0/0	
D248	0/2	0/0	
D150	0/2	0/0